Transportation Research Part C 147 (2023) 104009

Contents lists available at ScienceDirect

Transportation Research Part C

journal homepage: www.elsevier.com/locate/trc

Co-optimization of charging scheduling and platooning for long-haul electric freight vehicles

Md Rakibul Alam, Zhaomiao Guo[1,*]

Department of Civil, Environmental and Construction Engineering Resilient, Intelligent, and Sustainable Energy Systems Cluster University of Central Florida, FL 32766, United States of America

ARTICLE INFO

Keywords:
Electric freight vehicles
Charging scheduling
Mixed integer linear programming
Platooning
Long-haul freight transportation

ABSTRACT

Freight mileages have been significantly increasing over the past decade, accounting for 11% of global greenhouse gas (GHG) emissions. Freight electrification and platooning are two promising technologies to mitigate the energy and environmental impacts of freight transportation. Effective coordination of charging and platooning are urgently needed to maximize the benefits of these two technologies, especially considering the current inadequate charging infrastructure, long charging duration, higher energy usage, and tight delivery schedules for long-haul electric freight vehicles (EFVs). In this study, we aim to co-optimize the platooning and charging strategies of EFVs. To achieve this goal, we developed a mixed-integer linear programming model to minimize the total system costs, including en-route charging cost, delivery delay cost, and hub charging cost. The proposed model was tested using a case study of a 595-mile Florida interstate highway route and solved by the state-of-the-art branch-and-cut algorithms, through which we demonstrated the effectiveness of using our model to identify the optimal charging and platooning schedules and quantify the spatial distribution of charging demand and platoon energy savings. We also performed sensitivity analyses to better understand the impacts of some critical factors, including the EFV models, charging station (CS) capacity, number of CSs, charging speed, and departure-time windows.

1. Introduction

With the rapid development of e-commerce, freight mileages have been significantly increasing over the past decade, accounting for 11% of global greenhouse gas (GHG) emissions (MIT, 2021). In the United States, medium and heavy-duty trucks account for 23% of the GHGs emitted by the transportation sector (EPA, 2018). Long-haul trips, while representing only less than 1% of daily freight trips in frequency, account for more than 23% of the total vehicle miles traveled (VMT) and their impacts on energy and the environment are significant (Xie and Lin, 2021).

Freight electrification and platooning are two promising technologies being actively developed to mitigate the energy and environmental impacts of the long-haul freight sector (Zhou and Rood, 2019; Wang et al., 2019). However, each technology faces its own challenges in the freight sector. While car manufacturers are continuously extending the battery capacity of heavy-duty EFVs (e.g., Tesla Semi and Rivian R1T), due to the comparatively high payload, long charging duration, and sparse charging opportunities, long-haul EFVs require to meticulously schedule charging activities to ensure on-time delivery with minimum costs incurred from energy consumption and potential delivery delay (Smith et al., 2020). Platooning, enabled by vehicle-to-X (V2X) technologies, can

* Correspondence to: 4353 Scorpius Street, Orlando, FL 32816-0120, United States of America.
E-mail address: guo@ucf.edu (Z. Guo).
[1] Assistant Professor.

https://doi.org/10.1016/j.trc.2022.104009
Received 7 May 2022; Received in revised form 10 November 2022; Accepted 24 December 2022
Available online 30 December 2022

reduce energy consumption and charging needs by forming close-space groups of vehicles to reduce aerodynamic drag. In a platoon, the lead vehicle can save up to 10% at the closest separation distances, the middle vehicle up to 17%, and the trailing vehicle up to 13% (Lammert, 2020). However, only 63% of truck miles in the U.S. are platoonable given the condition that trucks need to travel at a minimum of 50 mph for at least 15 consecutive minutes together (Lammert et al., 2018). Additional charging needs of EFVs may further hamper the feasibility of forming platoons.

Although the long charging duration of electric freight vehicles (EFVs) may delay the shipment and the platooning requires perfect coordination between trucks' travel schedules over space and time, there is a great opportunity if we can co-optimize these two technologies. On one hand, the energy saving by platooning will significantly reduce the need for en-route charging and avoid shipment delays. On the other hand, EFVs' charging activities provide flexibility for them to coordinate their spatio-temporal trajectories, which offers more opportunities for EFVs to platoon.

In this paper, we explore the opportunities of leveraging charging duration to better coordinate platoon formation and leveraging platooning to reduce charging needs. The goal is to optimize the charging and platooning schedules of long-haul EFVs to minimize the total system costs. To achieve this goal, we developed a mixed integer linear programming (MILP) model to minimize the total system costs incurred from en-route charging, delivery delay, and hub charging. In addition, we conducted sensitivity analyses to investigate the impacts of the number of CSs, charging speed, and different departure times on the system costs. The main contribution of this paper is two-fold: (1) we developed an optimization model to co-optimize the scheduling of charging and platooning for long-haul EFVs; (2) we compared the state-of-the-art computational algorithms, including CPLEX's dynamic search algorithm, bender's decomposition algorithm, and branch-and-cut algorithm. To our best knowledge, this study is among the first to study the optimal operational strategies of integrated charging scheduling and platooning for long-haul EFVs. The model developed in this study can be an effective tool for the government to better understand the potential of integrating charging and platooning for EFVs; and for freight companies to schedule charging and platooning of an EFV fleet to optimize economic benefits and improve operational feasibility.

The remainder of this paper is organized as follows. Section 2 reviews the relevant literature on the scheduling of charging and platooning for EFVs. Section 3 explains the formulation of the MILP model. Section 4 presents the numerical results and analyses, including the details of the input for the case study (Section 4.1), comparisons of different algorithms to solve the model efficiently (Section 4.2), and the results from the case study and sensitivity analysis (Section 4.3). Finally, Section 5 concludes the paper with the main research findings and future research directions.

2. Literature review

We start the literature review with an overview of the recent topics related to EFVs, followed by the studies on charging scheduling and platooning issues for EFVs.

Existing literature has investigated the impacts of EFVs adoption in transportation systems. For example, Osieczko et al. (2021) and İmre et al. (2021) studied the potential benefits of introducing EFVs in the transportation sector with consideration of environmental emissions. Vijayagopal and Rousseau (2021) studied the economic benefits of EFVs in the road transportation sector. Nykvist and Olsson (2021) and Sen et al. (2017) investigated the necessity of battery improvement and the competitiveness of EFVs with conventional diesel-fueled trucks. The related transportation policies were also studied to better promote EFV adoption (Taefi et al., 2016).

EFVs can be used for both short-haul and long-haul delivery services in freight logistics systems. Short-haul delivery includes last-mile logistics from the distribution center to either customer's home or pickup point (Bosona, 2020). Long-haul delivery includes middle-mile delivery which typically transports freight between the retailer's warehouses or from the retailer's warehouse/distribution center to its retail store. Extensive EFV studies are found for last-mile logistics (Macrina et al., 2019; Anderluh et al., 2021; Basso et al., 2019; Klumpp et al., 2014; Bosona, 2020), with a focus on vehicle routing problems. The key parameters and assumptions that were considered in these studies included characteristics of energy consumption: deterministic or stochastic (Bruni et al., 2020), and charging strategy: full charging (Hiermann et al., 2016; Schneider et al., 2014; Andelmin and Bartolini, 2017) or partial charging at CSs (Desaulniers et al., 2016), charging location: only at a depot (Pelletier et al., 2019) or en-route charging (Bruni et al., 2020).

However, the studies on EFVs charging scheduling are still limited. For example, Bruni et al. (2020) considered the CS scheduling only for the single electric vehicle. Hiermann et al. (2016) and Andelmin and Bartolini (2017) restricted that an EFV is charged to full capacity at a CS regardless of their delivery constraints. Schneider et al. (2014) decided the optimal route where the optimal location and duration of charging were not identified. In addition, these studies do not consider long-haul delivery.

Among the previously mentioned charging-scheduling literature, different heuristics and exact algorithms were proposed to solve the models. For example, Hiermann et al. (2016) proposed a hybrid heuristic approach to solve the model instance which combined adaptive large neighborhood search and local search algorithms. Similarly, Schneider et al. (2014) proposed a hybrid heuristic approach that combined variable neighborhood search and tabu search algorithms. Andelmin and Bartolini (2017) implemented an exact algorithm that is based on set partitioning formulation with additional cuts. However, these studies did not solve the "co-optimization" problem for scheduling charging and platooning for long-haul EFVs. In addition, a comparison of the state-of-the-art algorithms is not found.

The methodologies for short-haul charging scheduling may not be directly transferable to long-haul EFVs because of dramatically different operational characteristics, including driver shifts, energy consumption, availability of charging infrastructure, and delivery constraints. For example, short-haul EFVs have comparatively less charging demand which causes the tendency to charge the EFVs

at the depot (Dalmijn et al., 2020). In addition, unlike the availability of CSs in the urban setting, the CSs are usually located sparsely for long-haul freight (Bischoff et al., 2019). Besides EFVs, the widely studied charging scheduling problem for passenger EVs cannot be directly leveraged because of the distinct charging behavior such as overnight home charging (Morrissey et al., 2016; Siddique et al., 2022) and charging at destination parking locations (Chen et al., 2013; Siddique et al., 2022). In addition, passenger EVs may not have strict travel schedules whereas long-haul FEVs have time windows for delivery they need to fulfill.

On the other hand, extensive research was undertaken to understand the advantages of platooning in fuel saving. Results show that the potential of fuel savings from platoons ranges from 5% to 20% (Alam, 2014; Bonnet and Fritz, 2000; Davila et al., 2013; Tsugawa, 2013) due to the improved aerodynamics of the platooned vehicles depending on their positions (Michaelian et al., 2000). In the context of platoon scheduling, Lee et al. (2021) developed a mathematical optimization model to determine the optimal configuration of platoons for a heterogeneous fleet of EFVs. The objective was to maximize the advantages of platooning including energy-saving and CO_2 emission reduction. However, this study did not consider charging for the vehicles.

The recent studies on charging scheduling for platooned vehicles have considered wireless CS which cannot resemble the system characteristics of the plug-in CSs. For example, Liu et al. (2019) developed a model to match vehicle platoons for platoon-based charging. Another study Zhang et al. (2021) proposed a charging scheme at signalized intersections. These EFVs leveraged the benefit of traffic signal's cycle time for wireless charging which is not applicable for long-haul EFVs.

In summary, the majority of EFVs studies focused either on charging scheduling or platoon coordination in last-mile freight transportation. Although the studies on wireless charging for platoon-based EFVs are found recently, the methodology cannot be transferred because of different system operational characteristics. To our best knowledge, this study is among the first to co-optimize both charging and platoon scheduling for long-haul freight transportation.

3. Methodology

3.1. Problem statement

On one hand, long-haul EFVs need to spend long charging time along the route, which can provide flexibility for platooning coordination. On the other hand, the platooning of EFVs reduces the total energy consumption, which can effectively save the en-route charging time. Therefore, the problem of interest in this study is to explore the optimal charging and platooning strategies for a fleet of EFVs when they travel through a long-haul route[2] to minimize the total cost incurred from en-route charging, hub charging and delivery delay. Charging scheduling determines the time, location, and duration for en-route charging while platooning scheduling determines when and where a vehicle entering/leaving a platoon.

3.2. Model formulation

To formulate this problem, we developed a mixed integer linear programming (MILP) model (1). The decision variables $t^{\text{arr}}_{j,s}$ decides when a vehicle j arrives at a charging station s and $t^{\text{cha}}_{j,s}$ decides the duration of charging time. Besides these charging scheduling decision variables, the platoon scheduling decision variable $y_{i,j,s}$ decides if a vehicle j joins platoon i or not at charging station s. The notation of all sets, variables, and parameters are described before the MILP model formulation. In addition, the detailed explanation of the MILP model including the objective function and the constraints are presented in Sections 3.2.1 and 3.2.2, respectively.

Note that we focus on deterministic modeling in this paper because of the following reasons. First, this study focuses on day-ahead planning of charging and platooning scheduling, instead of real-time operation. The value of this model is to determine possible platooning opportunities based on the day-ahead shipment schedules, which will need to be adjusted in a real-time operation based on the actual uncertainty realization. This is also the reason we keep the time resolution in our model at 30-min since higher resolution will further increase computational complexity and is unnecessary considering potential traffic congestion and randomness of freight operations. Second, extending the model to a stochastic version is straightforward using methods such as multi-stage stochastic programming or robust optimization. However, developing a stochastic model may require quantification of probability distributions or moments of the uncertain parameters, which are non-trivial tasks for rare events like traffic accidents and vehicle failures, and we leave it for future dedicated studies. Third, to our best knowledge, our study is among the first study on the co-optimization of charging and platoon scheduling. We keep our model deterministic to keep a clear focus, while still making valuable contributions to the literature in terms of mathematical modeling and computation of co-optimizing charging and platooning.

sets

$\mathcal{S}$: set of CSs; $\mathcal{S}' \doteq \mathcal{S} \bigcup \{O, D\}$

$\mathcal{S}_{\mathbf{gk}}$: set of CSs in the kth segments of the route that require driving break;

$\mathcal{J}$: set of vehicles;

[2] "Long-haul route" is identified as the route when an EFV requires en-route charging at least once.

$\mathcal{I}$: set of platoons;

$\mathcal{T}$: set of timestamps;

$\mathcal{K}$: set of segments that require driving break;

variables

$y_{i,j,s}$: vehicle j joins platoon i at station s, $\forall s \in \mathcal{S}'$;

$t^{\mathbf{dep}}_{j,s}/t^{\mathbf{arr}}_{j,s}$: time of vehicle j departs/arrives at station s, $\forall s \in \mathcal{S}'$;

$t^{\mathbf{dep}}_{i,s}/t^{\mathbf{arr}}_{i,s}$: time of platoon i departs/arrives at station s, $\forall s \in \mathcal{S}'$;

$soc^{\mathbf{dep}}_{j,s}/soc^{\mathbf{arr}}_{j,s}$: state-of-the-charge of vehicle j departs/arrives at station s, $\forall s \in \mathcal{S}'$;

$t^{\mathbf{cha}}_{j,s}$: charging time of vehicle j at station s, $\forall s \in \mathcal{S}$;

$t^{\mathbf{wait}}_{j,s}$: wait time of vehicle j at station s, $\forall s \in \mathcal{S}$;

$w_{i,s}$: binary variable if there is a platoon i at CS s $\forall s \in \mathcal{S}'$;

$c^{\mathbf{1}}_{j,s,\tau}$: indicator variable if a vehicle j arrives at CS s at timestamp τ, $\forall s \in \mathcal{S}$;

$c^{\mathbf{2}}_{j,s,\tau}$: indicator variable if a vehicle j charges at CS s at timestamp τ, $\forall s \in \mathcal{S}$;

$c_{j,s,\tau}$: indicator variable if a vehicle j both arrives and charges at CS s at timestamp τ, $\forall s \in \mathcal{S}$;

$b^{crash}_{j,s,s+1}$: indicator variable if vehicle j enters the link connecting CS s to $s+1$ within the accident impact time;

$z^1_{j,s}$: indicator variable if the departure time of vehicle j is greater than $t^{\text{crash}}_{s,s+1}$;

$z^2_{j,s}$: indicator variable if the departure time of vehicle j is less than $t^{\text{crash}}_{s,s+1} + t^{\text{impact}}$;

parameters

d_{s_1,s_2} : the distance between station s_1 and s_2, $\forall s_1, s_2 \in \mathcal{S}'$;

m_j : energy efficiency (kWh/mile) for vehicle j;

v_j : average speed of vehicle j;

v_i : average speed of platoon i;

$b^{\mathbf{c}}_j$: battery capacity of EFV j in kWh;

$r^{\mathbf{cha}}_s$: charging speed in kW at station s;

$t^{\mathbf{dep,min}}_j/t^{\mathbf{dep,max}}_j$: minimum/maximum departure time of vehicle j;

$t^{\mathbf{arr,\ max}}_j$: latest arrival time of vehicle j;

$t^{\mathbf{rest,\ min}}_j$: minimum rest time for vehicle j;

t_τ : time of a day for timestamp index τ;

$SOC^{\mathbf{dep}}_j/SOC^{\mathbf{arr,\ min}}_j$: departure/minimum arrival SOC of vehicle j;

$SOC^{\mathbf{min}}_j/SOC^{\mathbf{max}}_j$: minimum/maximum allowed SOC of vehicle j;

M : big number (to ensure a tight formulation, we select $M = 24$ for this study);

$\delta_{i,s}$: percentage of energy saving of platoon i departing from station s;

$c_s^{\mathbf{cha}}$: charging cost per kWh at station s;

$c_j^{\mathbf{delay}}$: delivery delay cost for vehicle j;

$c_j^{\mathbf{e}}$: energy (electric) cost for vehicle j when charge at depots;

$N^{\mathbf{max}}$: maximum number of vehicles allowed in a platoon;

n_s : maximum number of plugs in a CS s;

$t_{s,s+1}^{\mathbf{crash}}$: time of the occurrence of an accident between charging stations s and $s+1$;

$t^{\mathbf{impact}}$: time duration of crash impact;

$$\underset{y,w,t}{\text{minimize}} \quad \sum_{j\in\mathcal{J}}\sum_{s\in\mathcal{S}} c_s^{\text{cha}} r_s^{cha} t_{j,s}^{\text{cha}} + \sum_{j\in\mathcal{J}} c_j^{\text{delay}} (t_{j,D}^{\text{arr}} - t_j^{\text{arr,max}})^+ + \sum_{j\in\mathcal{J}} c_j^{\text{e}} [\sum_{s\in\mathcal{S}\bigcup O} d_{s,s+1} m_j (1 - \sum_{i\in\mathcal{I}} \delta_{i,s} y_{i,j,s}) - \sum_{s\in\mathcal{S}} r_s^{cha} t_{j,s}^{\text{cha}}] \tag{1a}$$

$$\text{s.t.} \quad soc_{j,O}^{\text{dep}} = SOC_j^{\text{dep}}; \quad \forall j \in \mathcal{J} \tag{1b}$$

$$soc_{j,D}^{\text{arr}} \geq SOC_j^{\text{arr,min}}; \quad \forall j \in \mathcal{J} \tag{1c}$$

$$soc_{j,s}^{\text{dep}} = soc_{j,s}^{\text{arr}} + \frac{r_s^{cha}}{b_j^c} t_{j,s}^{\text{cha}}; \quad \forall j \in \mathcal{J}, s \in \mathcal{S} \tag{1d}$$

$$soc_{j,s+1}^{\text{arr}} = soc_{j,s}^{\text{dep}} - \frac{d_{s,s+1} m_j}{b_j^c} (1 - \sum_{i\in\mathcal{I}} \delta_{i,s} y_{i,j,s}); \quad \forall j \in \mathcal{J}, s \in \mathcal{S}\bigcup\{O\} \tag{1e}$$

$$soc_{j,s}^{\text{arr}} \geq SOC_j^{\min}; \quad \forall j \in \mathcal{J}, s \in \mathcal{S} \tag{1f}$$

$$soc_{j,s}^{\text{dep}} \leq SOC_j^{\max}; \quad \forall j \in \mathcal{J}, s \in \mathcal{S} \tag{1g}$$

$$-M(1 - c_{j,s,\tau}^1) \leq t_\tau - t_{j,s}^{\text{arr}} \leq M c_{j,s,\tau}^1; \quad \forall j \in \mathcal{J}, s \in \mathcal{S}, \tau \in \mathcal{T} \tag{1h}$$

$$-M(1 - c_{j,s,\tau}^2) \leq t_{j,s}^{\text{arr}} + t_{j,s}^{\text{cha}} - t_\tau \leq M c_{j,s,\tau}^2; \quad \forall j \in \mathcal{J}, s \in \mathcal{S}, \tau \in \mathcal{T} \tag{1i}$$

$$-M(1 - c_{j,s,\tau}) \leq c_{j,s,\tau}^1 + c_{j,s,\tau}^2 - 1.5 \leq M c_{j,s,\tau}; \quad \forall j \in \mathcal{J}, s \in \mathcal{S}, \tau \in \mathcal{T} \tag{1j}$$

$$\sum_{j\in\mathcal{J}} c_{j,s,\tau} \leq n_s; \forall s \in \mathcal{S}, \tau \in \mathcal{T} \tag{1k}$$

$$t_{j,s}^{\text{dep}} = t_{j,s}^{\text{arr}} + t_{j,s}^{\text{cha}} + t_{j,s}^{\text{wait}}; \quad \forall j \in \mathcal{J}, s \in \mathcal{S} \tag{1l}$$

$$\sum_{s\in\mathcal{S}_{\text{gk}}\subset\mathcal{S}} (t_{j,s}^{\text{dep}} - t_{j,s}^{\text{arr}}) \geq t_j^{\text{rest,min}}; \quad \forall j \in \mathcal{J}, k \in \mathcal{K} \tag{1m}$$

$$t_j^{\text{dep,min}} \leq t_{j,O}^{\text{dep}} \leq t_j^{\text{dep,max}}; \quad \forall j \in \mathcal{J} \tag{1n}$$

$$t_{j,s+1}^{\text{arr}} = t_{j,s}^{\text{dep}} + d_{s,s+1}/v_j; \quad \forall j \in \mathcal{J}, s \in \mathcal{S}\bigcup\{O\} \tag{1o}$$

$$t_{i,s+1}^{\text{arr}} = t_{i,s}^{\text{dep}} + d_{s,s+1}/v_i; \quad \forall i \in \mathcal{I}, s \in \mathcal{S}\bigcup\{O\} \tag{1p}$$

$$t_{i,s}^{\text{dep}} = t_{i,s}^{\text{arr}}; \quad \forall i \in \mathcal{I}, s \in \mathcal{S} \tag{1q}$$

$$-M(1 - y_{i,j,s}) \leq t_{j,s}^{\text{dep}} - t_{i,s}^{\text{dep}} \leq M(1 - y_{i,j,s}); \quad \forall i \in \mathcal{I}, j \in \mathcal{J}, s \in \mathcal{S}\bigcup\{O\} \tag{1r}$$

$$\sum_{i\in\mathcal{I}} y_{i,j,s} \leq 1; \quad \forall j \in \mathcal{J}, s \in \mathcal{S}\bigcup\{O\} \tag{1s}$$

$$\sum_{j\in\mathcal{J}} y_{i,j,s} \leq w_{i,s} N^{\max}; \quad \forall i \in \mathcal{I}, s \in \mathcal{S}\bigcup\{O\} \tag{1t}$$

$$\sum_{j\in\mathcal{J}} y_{i,j,s} \geq 2w_{i,s}; \quad \forall i \in \mathcal{I}, s \in \mathcal{S}\bigcup\{O\} \tag{1u}$$

$$y_{i,j,s} \in \{0,1\}; \quad \forall i \in \mathcal{I}, j \in \mathcal{J}, s \in \mathcal{S}\bigcup\{O\} \tag{1v}$$

$$w_{i,s} \in \{0,1\}; \quad \forall i \in \mathcal{I}, s \in \mathcal{S}\bigcup\{O\} \tag{1w}$$

$$c_{j,s,\tau}^1, c_{j,s,\tau}^2, c^{j,s,\tau} \in \{0,1\}; \quad \forall j \in \mathcal{J}, s \in \mathcal{S}, \tau \in \mathcal{T} \tag{1x}$$

$$t_{j,s}^{\text{cha}}, t_{j,s}^{\text{wait}}, t_{j,s}^{\text{dep}}, t_{j,s}^{\text{arr}} \in \mathbb{R}_+; \quad \forall j \in \mathcal{J}, s \in \mathcal{S} \tag{1y}$$

$$t_{i,s}^{\text{dep}}, t_{i,s}^{\text{arr}} \in \mathbb{R}_+; \quad \forall i \in \mathcal{I}, s \in S \tag{1z}$$

3.2.1. Objective function

Objective (1a) minimizes the total cost while traversing the route from origin r to destination s. The total cost includes the en-route charging cost, calculated as $\sum_{j\in\mathcal{J}}\sum_{s\in S} c_s^{\text{cha}} r_s^{cha} t_{j,s}^{\text{cha}}$, delivery delay cost, calculated as $\sum_{j\in\mathcal{J}} c_j^{\text{delay}}(t_{j,D}^{\text{arr}} - t_j^{\text{arr,max}})^+$, and hub charging cost, calculated as $\sum_{j\in\mathcal{J}} c_j^{\text{e}}[\sum_{s\in S\bigcup O} d_{s,s+1} m_j(1-\sum_{i\in\mathcal{I}}\delta_{i,s}y_{i,j,s}) - \sum_{s\in S} r_s^{cha} t_{j,s}^{\text{cha}}]$. In this paper, we assume that the total energy consumption of a vehicle needs to be charged at either en-route charging stations or at the depots. Therefore, the total charging costs should include both en-route charging costs (the second term) and hub charging costs (the last term). If one ignores the last term, the consequence is that vehicles will try to only minimize the en-route charging costs and do not care about the total energy consumption. In other words, the benefits of platooning, which reduce the total energy consumption, are not fully taken into account. Energy cost at depots, i.e., the hub charging cost, is formulated as

$$\sum_{j\in\mathcal{J}} c_j^{\text{e}}[\sum_{s\in S\bigcup O} d_{s,s+1} m_j(1-\sum_{i\in\mathcal{I}}\delta_{i,s}y_{i,j,s}) - \sum_{s\in S} r_s^{cha} t_{j,s}^{\text{cha}}]$$

Here, $\sum_{s\in S\bigcup O} d_{s,s+1} m_j(1-\sum_{i\in\mathcal{I}}\delta_{i,s}y_{i,j,s})$ is the total energy consumed for vehicle j considering the energy saving if the vehicle j joins a platoon. The charging demand from en-route charging stations, which is calculated as $\sum_{s\in S} r_s^{cha} t_{j,s}^{\text{cha}}$, needs to be deducted from the total energy consumption to estimate the energy that is still required to be charged at depots. The required charging energy at depots is multiplied by c_j^e to estimate the required charging costs at depots.

3.2.2. Constraints

State of charge (SOC)

Constraints (1b)–(1g) describe the dynamics of SOC of each vehicle j while traversing the route through CSs including origin and destination. Constraint (1b) and (1c) describes the departure SOC at the origin and minimum arrival SOC at the destination, respectively. The charging dynamics at CSs are specified in constraint (1d), in which the departure SOC at CS s is calculated as the arrival SOC at CS s plus the energy charged at this station. Constraint (1e) specifies the energy consumption along the route, i.e., the arrival SOC at the next CS equals the departure SOC at the previous CS minus the energy consumption in-between. Notice that the energy consumption between two consecutive CSs will depend on if the vehicle has joined a platoon or not. In this study, we assume an average energy saving if a vehicle joins a platoon regardless of vehicle position. The main reason for this assumption is that vehicles could belong to different freight companies and vehicles in a platoon may need to switch positions to guarantee the fairness of energy savings. Constraints (1f) and (1g) describe the minimum and maximum limits of SOC on arrival and departure at a CS, respectively. The minimum SOC aims to ensure sufficient energy buffers for EFVs and the longevity of vehicle batteries. Notice that constraints (1f) and (1g) also guarantee the SOC along the travel route to be within the specified maximum and minimum values because we do not consider wireless charging so that SOC can only decrease in-between CSs.

Capacitated charging stations

Constraints (1h)–(1k) ensure the charging dynamics based on the capacity of charging stations. In constraint (1h) and (1i), the arrival state and charging state of vehicle j at CS s at time τ is tracked for each timestamp by binary variables $c_{j,s,\tau}^1$ and $c_{j,s,\tau}^2$, respectively. We use binary variables $c_{j,s,\tau}^1$ and $c_{j,s,\tau}^2$ to indicate that if the vehicle has arrived (constraint (1h)) and charged (constraint (1j)) at timestamp τ. For example, if $c_{j,s,\tau}^1 = 1$ and $c_{j,s,\tau}^2 = 1$, constraints (1h) and (1i) become $0 \le t_\tau - t_{j,s}^{arr} \le M$ and $0 \le t_{j,s}^{arr} + t_{j,s}^{cha} - t_\tau \le M$, respectively, which represents that vehicle j has arrived at CS s at t_τ (i.e., $t_\tau \ge t_{j,s}^{arr}$) and have not finished charging (i.e., $t_\tau \le t_{j,s}^{arr} + t_{j,s}^{cha}$). Constraint (1j) specifies whether a vehicle both arrives and charges at a CS at a particular timestamp. In constraint (1j), we ensure that the binary variable $c_{j,s,\tau}$ will be 1 if and only if $c_{j,s,\tau}^1$ and $c_{j,s,\tau}^2$ are both equal to 1. When $c_{j,s,\tau}$ is 1, $0 \le c_{j,s,\tau}^1 + c_{j,s,\tau}^2 - 1.5 \le M$ based on constraint (1j). This means $c_{j,s,\tau}^1 + c_{j,s,\tau}^2 - 1.5$ should be non-negative, which is identical with both $c_{j,s,\tau}^1$ and $c_{j,s,\tau}^2$ equal to 1. We can also change 1.5 to any value within the range $(1, 2)$. At each timestamp, the total number of vehicles charging at a CS cannot exceed the capacity of the CS which is defined by constraint (1k).

Time

Constraints (1l)–(1r) describe the temporal constraints of each vehicle and platoon as well as the driver's rest time. In constraint (1l), the departure time of a vehicle from a CS is calculated as the arrival time at the CS plus the active charging time and the waiting time before joining a platoon. Constraint (1n) specifies the range of the earliest and latest departure times of each vehicle at the origin, which depends on the time when all the shipments are loaded. Notice that the departure time for different vehicles can also be pre-specified at a fixed time by setting $t_j^{\text{dep,min}} = t_j^{\text{dep,max}}$. Constraint (1o) calculates the arrival time of a vehicle at a CS as the departure time from the previous CS plus the time required to travel between the consecutive CSs. A minimum rest time is allotted to each driver per regulations of the freight industry for every given driving duration, as specified by constraint (1m). Rest time is bestowed upon the charging time and waiting time before joining a platoon. Similar to the arrival time of a vehicle at a CS, the arrival time of a platoon is defined by constraint (1p). Constraint (1q) indicates that the arrival and departure time of a platoon at a CS should be the same (i.e., a platoon will keep moving forward and vehicles can either join or leave the platoon) since a platoon cannot wait at a CS to allow individual vehicles in the platoon to charge. Notice that this constraint does not exclude the scenario that all the vehicles in one platoon need to charge at the same charging station and they will continue to platoon after

charging because the model can assign a new platoon index to represent the new platoon formed. Constraint (1r) indicates that if a vehicle joins a platoon (i.e., $y_{i,j,s} = 1$), the departure time of the vehicle and the platoon at the CS should be the same.

Platoon formation

Constraints (1s)–(1u) describe the requirements of platoon formation. Constraint (1s) describes that each vehicle can only join at most one platoon at a particular time. Constraints (1t)–(1u) specifies that for an activated platoon i at CS s (i.e., $w_{i,s} = 1$), it can contain a minimum of 2 and a maximum of $N^{\max}$ vehicles.

Variable types

Constraint (1v) specifies the binary type of one of the decision variables: $y_{i,j,s}$. In addition, constraints (1w) and (1x) specify the binary type of indicator variables: $w_{i,s}$, $c^1_{j,s,\tau}$, $c^2_{j,s,\tau}$ and $c_{j,s,\tau}$. Constraints (1y) and (1z) are the non-negative constraints for the decision variables associated with time for vehicles and platoons, respectively.

3.3. Remarks

To conclude the modeling session, we discuss two natural extensions that may further generalize the proposed model. First, we discuss how to re-optimize the charging and platooning scheduling in response to accidents, which can cause significant travel delays. Second, we discuss how to consider variable charging prices in our model.

3.3.1. Response to accidents

An accident may create a bottleneck on the road, which may reduce the speed of vehicles and increase the travel time of the long-haul trip. The delay will depend on how long the bottleneck takes to be removed and when the vehicle will arrive at the impacted area. Therefore, after an accident happens, the original planned charging and platooning schedules may not be feasible anymore and should be re-planned.

Assume an accident occurs at time $t^{\text{crash}}_{s,s+1}$ between charging stations s and $s+1$ and its impact time duration is t^{impact} hours. For any vehicle j enters the link connecting s and $s+1$ within t^{impact}, the vehicle j will have a slower average speed v'_j. We use binary variables $b^{crash}_{j,s,s+1}$ to indicate if vehicle j enters the link s to $s+1$ within the accident impact time, i.e. $[t^{\text{crash}}_{s,s+1}, t^{\text{crash}}_{s,s+1} + t^{\text{impact}}]$. To determine $b^{crash}_{j,s,s+1}$ within an optimization model, we need to add constraints (2a)–(2e). We create two additional auxiliary binary variables $z^1_{j,s}$ and $z^2_{j,s}$, which indicate if the departure time of vehicle j is greater than $t^{\text{crash}}_{s,s+1}$ and less than $t^{\text{crash}}_{s,s+1} + t^{\text{impact}}$, as shown in (2a) and (2b), respectively. If both $z^1_{j,s}$ and $z^2_{j,s}$ equal to 1, then $b^{crash}_{j,s,s+1}$ is 1, as constrained by (2c)–(2e).

$$t^{\text{dep}}_{j,s} - t^{\text{crash}}_{s,s+1} \le M z^1_{j,s}; \quad \forall j \in \mathcal{J}, s \in \mathcal{S} \bigcup \{O\} \tag{2a}$$

$$t^{\text{crash}}_{s,s+1} + t^{\text{impact}} - t^{\text{dep}}_{j,s} \le M z^2_{j,s}; \quad \forall j \in \mathcal{J}, s \in \mathcal{S} \bigcup \{O\} \tag{2b}$$

$$b^{crash}_{j,s,s+1} \le z^1_{j,s}; \quad \forall j \in \mathcal{J}, s \in \mathcal{S} \bigcup \{O\} \tag{2c}$$

$$b^{crash}_{j,s,s+1} \le z^2_{j,s}; \quad \forall j \in \mathcal{J}, s \in \mathcal{S} \bigcup \{O\} \tag{2d}$$

$$b^{crash}_{j,s,s+1} \ge z^1_{j,s} + z^2_{j,s} - 1; \quad \forall j \in \mathcal{J}, s \in \mathcal{S} \bigcup \{O\} \tag{2e}$$

With variable $b^{crash}_{j,s,s+1}$, we can calculate the vehicle speed as $v_j = (1 - b^{crash}_{j,s,s+1}) v^0_j + b^{crash}_{j,s,s+1} v'_j$, where v^0_j is the base speed and v'_j is the speed with accidents. The remaining model does not need to be changed.

3.3.2. Variable charging prices

We note that extending our model to consider real-time electricity prices which vary over time but are known in advance is a straightforward process. In our model, we use parameter c^{cha}_s to represent the charging costs at charging station s, which can be further indexed by j, (i.e., $c^{\text{cha}}_{j,s}$) to reflect that different vehicle j could be charged differently depends on the time they plug-in. $c^{\text{cha}}_{j,s}$ can be calculated as $\sum_{\tau \in \mathcal{T}} c^{\text{cha}}_{s,\tau} c_{j,s,\tau}$, where $c^{\text{cha}}_{s,\tau}$ is known parameters indicating the unit charging cost at charging station s and timestep τ and $c_{j,s,\tau}$ indicates if the vehicle j charges at CS s in a particular timestamp τ.

4. Numerical examples

4.1. Inputs

To demonstrate the effectiveness of the proposed model, we retrieved the trip data of commercial freight trucks from the Florida container number database (CND) (FDOT, 2022). After processing 7-day trip data of commercial freight vehicles in Florida, we retrieved multiple origin–destination (OD) points and the fastest routes for these OD points based on OpenStreetMap as shown in Fig. 1. We selected the route from I-10 Pensacola (Node 0) to US-27 Hendry (Node 17) with a total length of 595 miles for the case study. In addition, considering a 1-mile buffer distance from this route, 16 DC fast-charging stations were identified based on the charging station data from Alternative Fuels Data Center (AFDC) (retrieved from https://afdc.energy.gov/data/ on Nov.15, 2021). Fig. 1 shows the case-study route in thick "blue" lines and CSs in diamond-shaped marks.

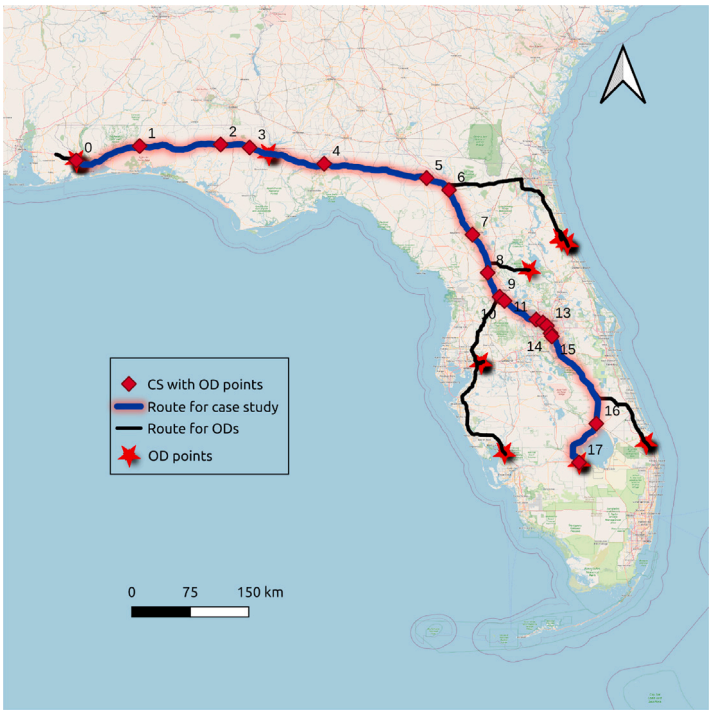

Fig. 1. Study-route. (For interpretation of the references to color in this figure legend, the reader is referred to the web version of this article.)

We implemented our model for this route given the parameter values as shown in Table 1. This study does not aim to optimize the scheduling for all heavy-duty trucks active in the network because of three main reasons. First, it is relatively impractical to assume that a central operator knows the delivery tasks of all trucks and is able to control their charging and platooning schedules because trucks are typically owned by private companies and information is not shared due to privacy and/or business considerations. Second, not all EFVs are eligible/suitable for platooning due to shorter trip distances and vehicle technologies. Third, the system operator may not need to consider all the vehicles that with distinct departure times (e.g., trucks depart in the morning and in the evening), since they have limited opportunities to platoon.

To estimate the scale of vehicle numbers serving for that specific OD, we used Container Number Database (CND) data from the Florida Department of Transportation (FDOT). This database collects spatial–temporal data of commercial heavy-duty trucks (gross weight > 26 000 lbs) at weigh stations in Florida. On average, 11 875 commercial heavy-duty trucks are active in Florida daily. However, the number of long-haul trucks that have a trip distance of more than 300 miles and 350 miles within a 24-h time window are found to be only 37 and 3, respectively. Therefore, in our numerical study settings, we consider a fleet size of 20 EFVs as a starting point to gain numerical insights into the potential benefits of co-optimizing charging and scheduling for a small fleet of EFVs. The earliest departure time was allowed from midnight. A fleet of EFVs was considered to have an identical configuration of batteries with a 300-miles range when loaded. The fuel efficiency was considered 1.5 kWh/mile based on the average fuel efficiency of state-of-the-art EFV models Tesla Semi, Rivian R1T, and Freightliner eCascadia. We assumed that vehicles can interchange their position within the platoon and each vehicle in the platoon will save on average 13% of energy consumption. In addition, we considered DC fast chargers with a 100 kW charging rate for the base case. According to Federal Motor Carrier Safety Administration (FMCSA), a break of at least 30 consecutive minutes is recommended for freight drivers after 8 cumulative hours of driving time (FMCSA, 2022). In our model, a minimum of 30-min rest was required for freight drivers in two halves of the entire route. In our test route, CSs 1–6 were the candidate resting area in the first half of the route and the remaining CSs were the resting area for the second half. The charging time and waiting time before joining a platoon can be counted toward the driver's rest time. We set the maximum number of platoons allowed the same as the number of EFVs, which would provide the maximum flexibility to form platoons since each platoon at least contains two EFVs. We also assume a speed of 50 mph for both individual vehicles and platoons. It was assumed that the battery of a vehicle was fully charged at the beginning of the trip, and the maximum and minimum SOCs were 100% and 20%, respectively. We also assumed it was cheaper to charge at the hubs ($0.1165/kWh) compared with en-route charging ($0.28/kWh). The delay cost was set to be $50/h.

The length of the time interval is important and should be selected in a way balancing the consideration of model accuracy and computational feasibility. That is the reason we choose $\tau = 30$ min considering the resolution requirements of the long-haul freight industry (e.g., drivers need to take at least a 30-min break every 8 h and delivery time windows are typically in the range of 1–2 h) and the computation complexity.

Table 1
Summary of parameters for the base case and sensitivity analysis.

	Unit	Base case	Sensitivity test
Number of vehicles	–	20	5,10,20
Allowable number of platoons	–	20	Unchanged
Number of CSs	–	16	3,5,8,16
Number of charging plugs	–	–	1-8 based on AFDC data
Fuel efficiency of vehicles	kWh/mile	1.5	1.4 (eM2),1.9 (eCascadia),2(Semi)
Battery capacity of vehicles	kWh	300	315 (eM2),475 (eCascadia),1000 (Semi)
Charging speed	kW	100 kW	25,50,75,100,350
Vehicle/Platoon speed	mph	50	Unchanged
Time to reach destination	h	17	Unchanged
Average energy saving in platoon	%	13	Unchanged
SOC at origin	%	100	Unchanged
Minimum SOC on arrival	%	20	Unchanged
Maximum SOC at departure	%	100	Unchanged
Charging cost	$/kWh	0.28	0.13,0.18,0.23,0.28
Home electricity cost	$/kWh	0.1165	Unchanged
Delay cost	$/h	50	Unchanged

Table 2
Comparison of computational times.

Number of EFVs	CPLEX default (Dynamic) search algorithm		Bender's decomposition algorithm		Branch-and-cut algorithm			
					Before tuning parameter		After tuning parameter	
	Computational time (s)	Optimality gap (%)	Computational time (s)	Optimality gap (%)	Computational time (s)	Optimality gap (%)	Computational time (s)	Optimality gap (%)
5	20	0	2004	0	27	0	1	0
10	494	0	>7200	21.22	658	0	11	0
15	4732	0	>7200	21.09	382	0	83	0
20	>7200	1.39	>7200	20.79	2224	0	725	0
25	>7200	12.99	>7200	31.65	2742	0	227	0

4.2. Computational performance

Model (1) is an NP-hard MILP optimization problem. We compared the computational time of three solution approaches (as shown in Table 2), including the dynamic search algorithm, the Bender's decomposition algorithm Appendix A, and the branch-and-cut algorithm Appendix B on test cases with different numbers of EFVs from 5 to 25. We implemented the model using CPLEX 20.1.0 (Cplex, 2020) Python API. All the experiments were run on an Intel(R) Core i9-9900K eight-core processor with 16 GB of RAM memory, under UBUNTU 18.04.2.

For the dynamic search algorithm, it was found that with a fleet size of 20 and 25, the model cannot be solved in 2 h, with an optimality gap of 1.39% and 12.99%, respectively. Bender's decomposition is a popular decomposition strategy for MILP with a particular block structure (Zhao et al., 2021). However, for our model, the computational time was longer even for small fleet sizes (optimality gap: 21.22% in 2 h for 10 EFVs only).

In contrast, branch-and-cut algorithms were found to be much faster than dynamic search and bender's decomposition algorithms. Branch-and-cut algorithms generate cuts to the branch-and-bound tree with the aim of improving the lower bound and producing "more integral" solutions (Gounaris et al., 2011). For a fleet size of 25 EFVs, the optimal solution was achieved in 2742 s with CPLEX default settings. The computation time was further improved by tuning only three default parameters of CPLEX. First, the parameter "MIP emphasis switch", which controls the trade-off between speed, feasibility, optimality, and moving bounds in MILP, was tuned to 4 (emphasis on finding hidden feasible solutions). Second, "cutpasses", which sets the upper limit of the number of cutting plane passes while solving the root node of the MILP model, was tuned to −1 (no cutting planes). Third, "probing", which sets the amount of probing on variables before MILP branching, was tuned to −1 (no probing). It was found that the branch-and-cut algorithm after tuning the parameters performed significantly better than the non-tuned branch-and-cut algorithm and became the best among all three algorithms we tested, as shown in Table 2. For example, 227 s were needed to solve the model for a fleet size of 25.

4.3. Results analyses

This section includes two parts. First, we present the base case results to investigate the optimal scheduling of charging/platooning and potential cost savings. Second, we present sensitivity analysis results to better understand the impacts of CS capacity, EFV technologies, charging speeds, number of CSs, and departure times on the system costs.

Table 3
Comparative results of with and without platooning.

	With platooning	No platooning
En-route charging energy (kWh)	10 729	13 050 (+22%)
En-route charging cost ($)	3004	3654 (+22%)
Hub charging energy (kWh)	4798	4798 (0%)
Hub charging cost ($)	559	559 (0%)
Delivery delay (h)	5.3	28.5 (+437%)
Delivery delay cost ($)	265	1425 (+437%)

4.3.1. Base case results

For the base case, the optimal en-route charging cost, delivery delay cost, and hub charging cost were found to be $3004.5, $265, and $559.2, respectively. Fig. 2 visualizes the scheduling of charging time and duration at CSs for each EFV. We found that each EFV chose to charge 3–6 times along the route. Multiple charging times help EFVs to better adjust their spatial–temporal locations so that they can join platoons easier to save energy consumption. The total amount of charging demand is the same for each EFV because of their identical battery configurations and efficiency and in the base case, all vehicles traverse the route in platoons. However, the decisions on the charging locations and duration for each charging session varied because of the need to coordinate with platoon formation. It was also found that most of the en-route charging demand was satisfied 3–9 h after the departure time from the origin. This could be because (1) EFVs do not have enough battery room to charge in the first two hours if they start with a fully charged battery; (2) relatively earlier charging decisions can allow them the opportunities to platoon early, which leads to more energy savings; (3) EFVs will be less likely to charge en-route when closer to the destination due to cheaper charging options at the destination.

The spatial charging demand distribution is shown in Fig. 3, in which we found that CS2, CS4, CS5, and CS15 had higher charging demand (>1000 kWh). We observed that CS2, CS4, and CS5 are located at a long distance away from their previous CS which is more than 60 miles. Therefore, there is a higher charging demand for these CSs. As a result, the immediate following CSs, which are within 23 miles, have less charging demand. It was also found that after satisfying a large amount of charging demand (1241 kWh) in CS5, the charging demand was less for the remaining CSs until CS15. As 9 charging stations are located between CS5 and CS15 which are very close to each other (average 21 miles) compared with CSs within CS1 to CS5 (average 55 miles interval), charging demand is spread out among these 9 CSs. Even though CS16 is 86.5 miles away from the previous CS15, the charging demand was not high. This might be because of two reasons. First, the high charging demand (1545 kWh) is already satisfied in CS15. Second, due to cheaper hub charging costs at the destination compared to en-route charging, EFVs will only charge the minimum amount en-route.

Fig. 4 visualizes the platooning progression throughout all CSs. We can see that at every charging station, all the 20 vehicles belong to one platoon, which means that no vehicle is driving by itself at any given time and location of the trip. The number of EFVs in each platoon at each CS changed in such a way that the total energy saving could be maximized while minimizing potential EFV delivery delay.

Importance of allowing platooning. The energy consumption at each segment of the route is mapped in Fig. 5, in which we compared the energy consumption for each segment between two cases: without platooning and with platooning. It was found that segments CSs 1–2, CSs 3–4, and CSs 6–7 had a significant reduction in energy consumption from platooning, which indicates less air pollution in the surrounding zones.

When we do not consider platooning, the vehicles need 22% additional en-route charging energy (13 050 kWh) compared with the case considering platooning (10 729 kWh), as shown in Table 3. This additional charging demand increases 21% of en-route charging time. Due to the increased en-route charging time, the delivery delay cost without platooning is $1425, which is 5.4 times the amount with platooning ($265). We found no change in hub charging demand because the additional energy has been satisfied by en-route charging to complete delivery. The energy demand (kWh) at each charging station is also illustrated in Fig. 5.

Importance of the combination of charging and platoon scheduling. We further compare the cases between considering and ignoring charging and platooning coordination. In the case of *ignoring charging and platooning coordination*, we assume that all vehicles will depart as early as possible when the shipment is loaded and charge en-route as late as possible to prevent the SOC falls below 20%. The EFVs will form platoons if they depart from the same charging station at the same time step. The route length, charging station information, battery configuration of the vehicles are kept the same as the base case.

It is found that if charging and platooning were not coordinated, all vehicles stopped at CS 3, 6 and 13 with battery SOC of 31.7%, 20%, and 24%. When vehicles reached the depot, the required hub charging energy was 219 kWh for each vehicle. The total energy cost was $5504, which is 44% higher than the total energy cost ($3827) when charging and platooning are coordinated. The detailed comparison is shown in Table 4.

4.3.2. Sensitivity analysis

We conducted sensitivity analyses to better understand the impact of different features: EFV models, departure time flexibility, the capacity of CSs, number of CSs, and charging speed on the system costs. The parameter settings are described in Table 1. We considered equal percentage distribution of three different models of EFVs which are Freightliner's eCascadia, eM2, and Tesla's

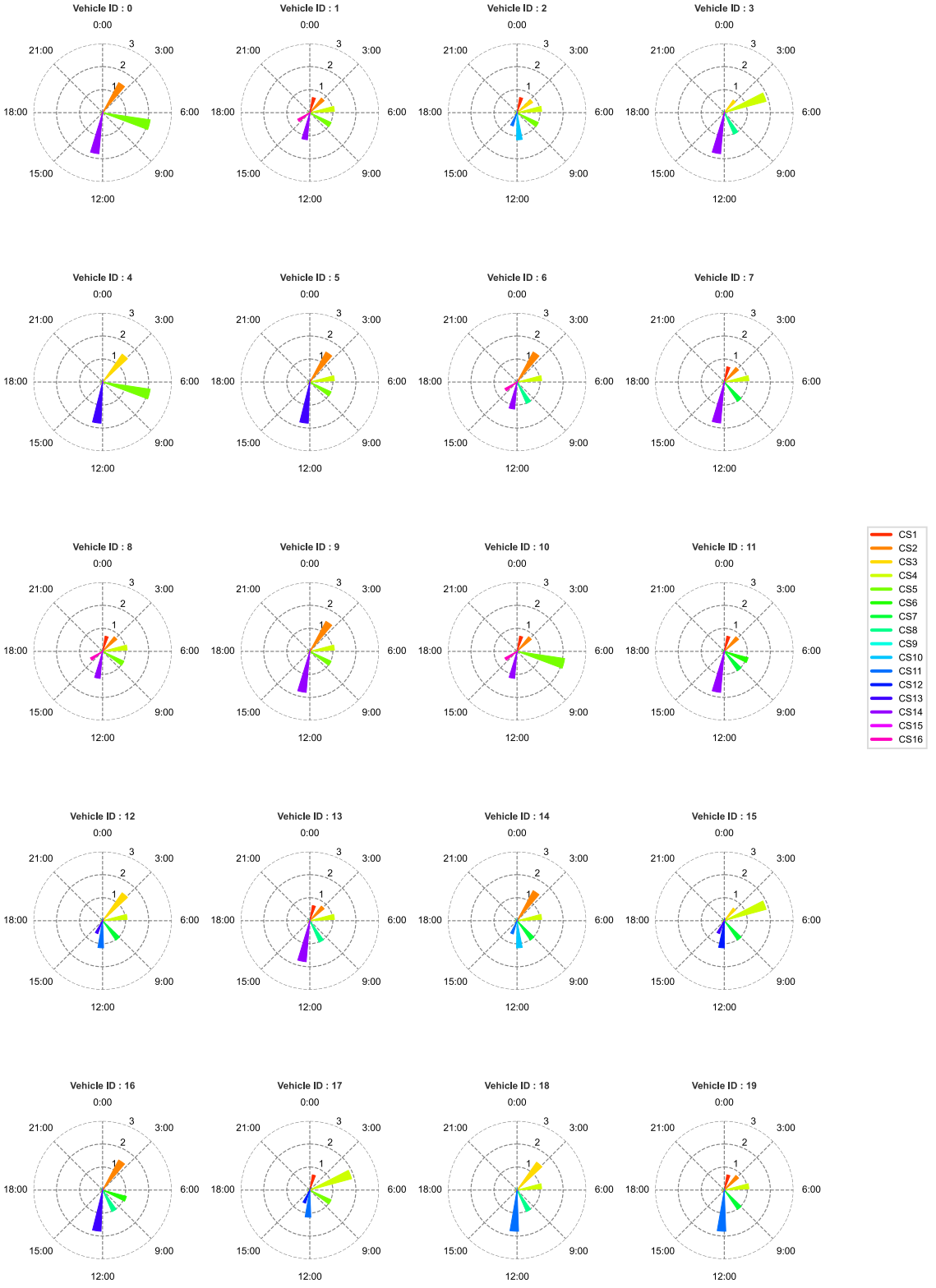

Fig. 2. Charging duration in hrs (along the radius of the polar plot) at different CSs in 24-h clock.

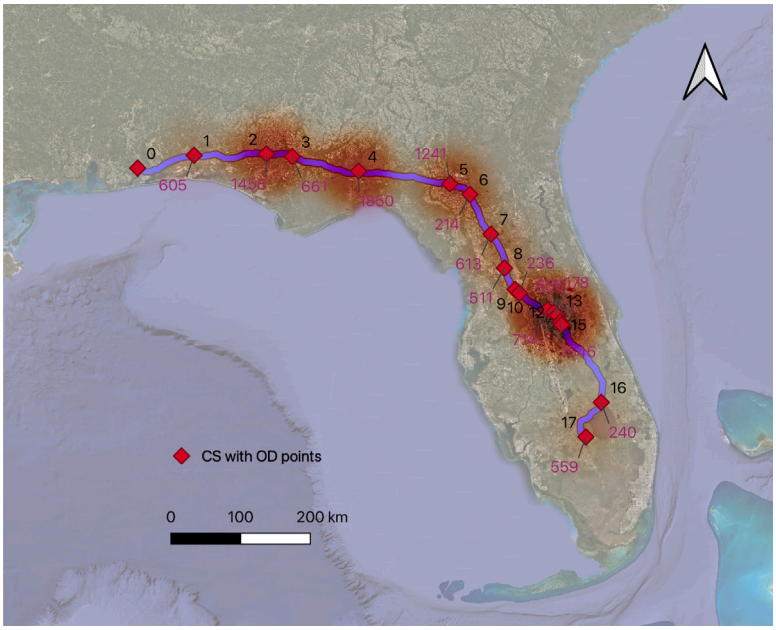

Fig. 3. Charging demand in CSs.

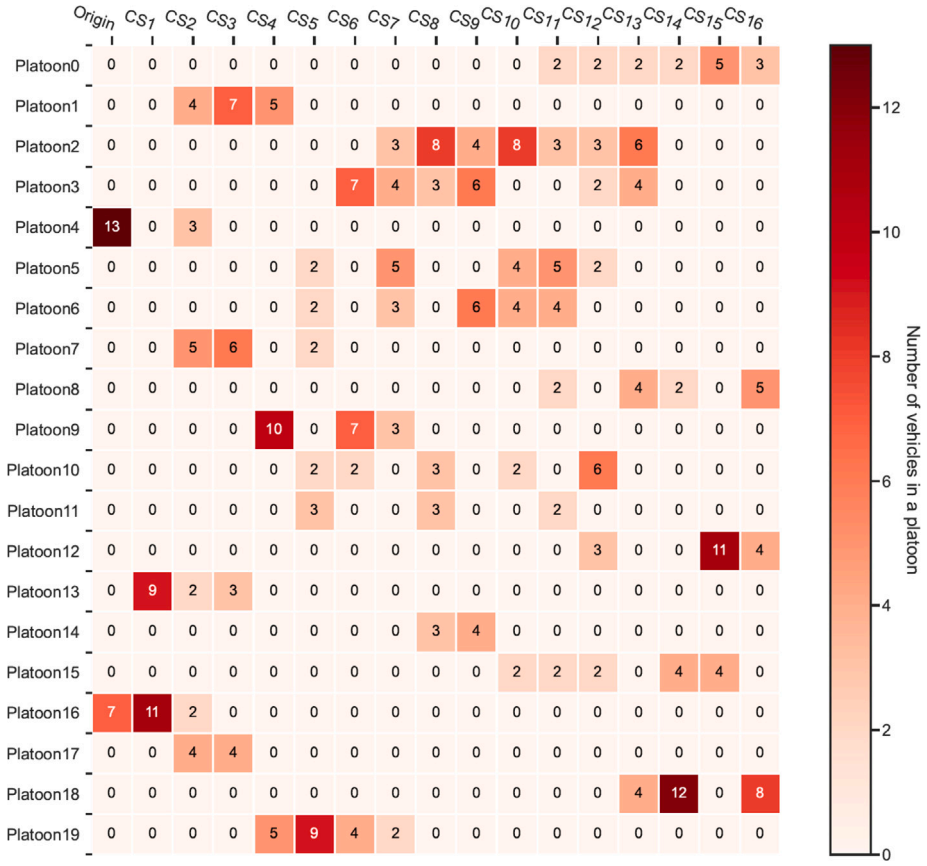

Fig. 4. Number of vehicles in each platoon at different CSs.

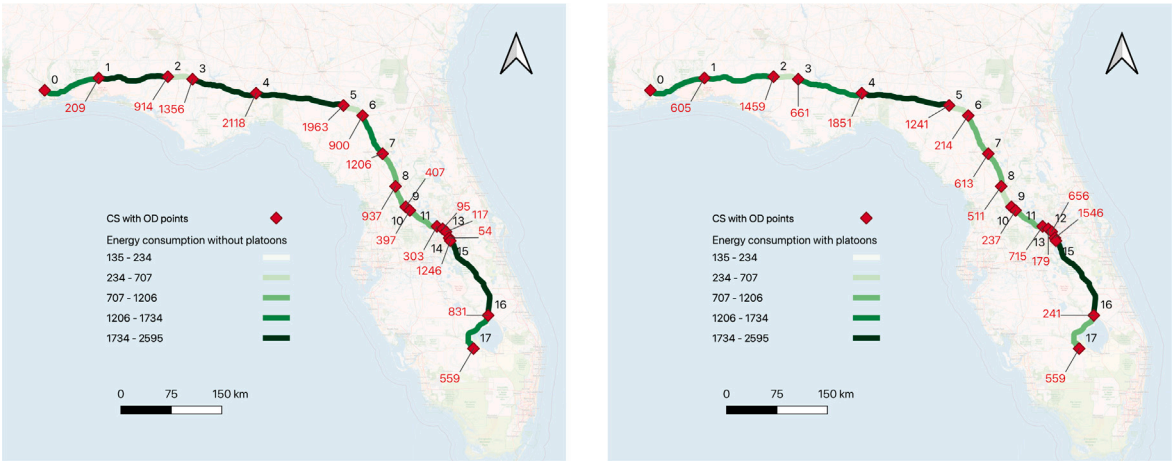

(a) Energy consumption without platoons (b) Energy consumption with platoons

Fig. 5. Energy consumption (kWh) on route segments and charging demand (kWh) in each CS.

Table 4
Comparative results between with and without charging and platooning coordination.

	Coordination	No coordination
En-route charging energy (kWh)	10 729	17 838 (+66%)
En-route charging cost ($)	3004	4994 (+66%)
Hub charging energy (kWh)	4798	4380 (−9%)
Hub charging cost ($)	559	510 (−9%)
Delivery delay (h)	5.3	0 (−100%)
Delivery delay cost ($)	265	0 (−100%)

Semi as EFVs with battery capacity >300 kWh for the sensitivity test of battery capacity. The EFVs with 300 kWh were considered according to the base-case setting and in addition, EFVs with 150 kWh were also considered in the sensitivity test of battery capacity. Two scenarios of the departure time of EFVs: model-decided departure time and randomly selected from the first 4-h time windows with a random seed value of 123. For sensitivity analyses of CS numbers, two scenarios of 5 and 10 equidistant CSs with an equal capacity of 3 charging plugs were considered for 5 EFVs. For sensitivity analyses of CS capacity, the number of charging plugs was collected from the AFDC data repository in the capacitated CS scenario, while the uncapacitated CS scenario does not have a charging-plug limitation. 10 EFVs were considered in the CS capacity sensitivity analyses. In addition, to better understand the sensitivity of time resolution on computational efficiency and delivery delay, we compare two time intervals: 15 min and 30 min. Since the charging speed is not linear for DCFC, a common practice for EFV charging is to cap the SOC at 80% to avoid overheating and maintain proper charging speed. We further compare the results between the cases with 80% and 100% SOC. Different levels of charging speeds: 25, 50, 75, 100, and 350 kW were considered for the sensitivity analyses of charging speed (Kavianipour et al., 2021). The results are shown in Fig. 6.

Departure time from origin. The impacts of fixed departure time and flexible departure time of each vehicle on charging costs are illustrated in Fig. 6(a). When the model could freely choose the departure time of EFVs during a day, the departure time of all the EFVs was set at the beginning of the day, which resulted in a huge saving in delivery delay costs. When the departure time of EFVs was randomly given, the EFVs still have the same total charging energy/time and delivery time requirements, which results in a larger delivery delay cost. From Fig. 6(a), we also observe that the en-route and hub charging costs are insensitive to departure time. This is because although vehicles have different departure times, they are still able to join platoons throughout their trips to save the same amount of energy consumption, resulting in unchanged en-route and hub charging needs.

Battery capacity. The impacts of EFVs with different battery capacities on charging costs are illustrated in Fig. 6(b). We found that EFVs with higher battery capacity decreased en-route charging costs and delivery delay costs, while increased hub charging costs, compared with EFVs with lower battery capacity. For example, EFVs with a battery capacity of 150 kWh are 22% higher in the en-route charging cost, 5.5 times more delivery delay costs, and 50% lower hub charging costs, compared with EFVs with >300 kWh battery. The reason is that EFVs with lower battery capacity have higher en-route charging needs to traverse the route. Higher charging needs will cause more en-route charging time, which will result in higher delivery delay costs. But since the total energy consumption for all of the EFVs is similar, EFVs with higher battery capacity will prefer to charge more at the destination, which has a cheaper energy price than en-route charging.

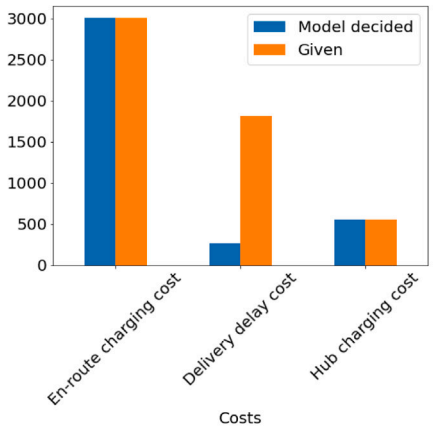

(a) Costs for different departure-time types

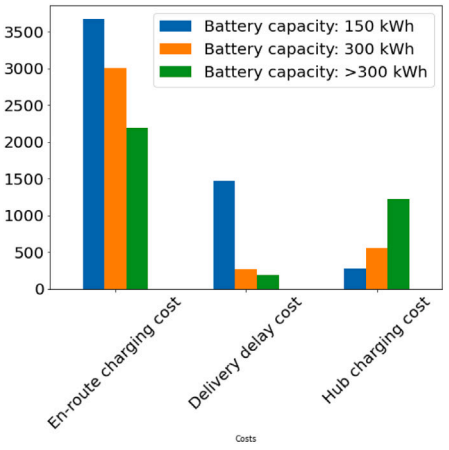

(b) Costs for EFVs with different battery capacities

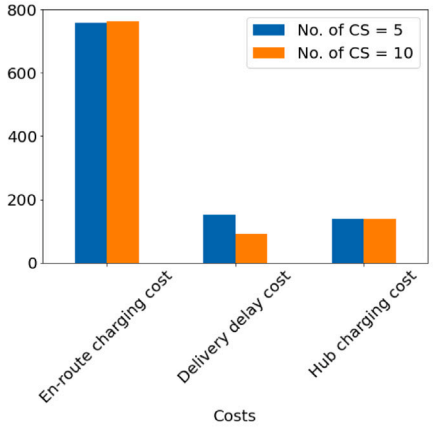

(c) Costs for different numbers of CSs

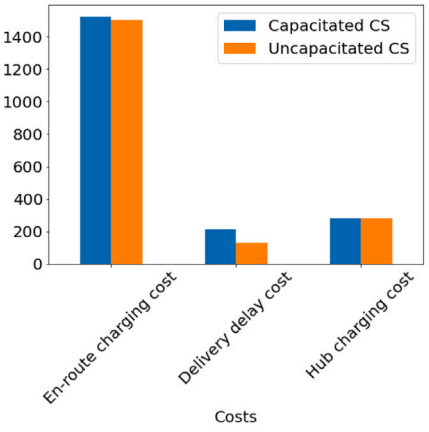

(d) Costs for capacitated and uncapacitated CSs

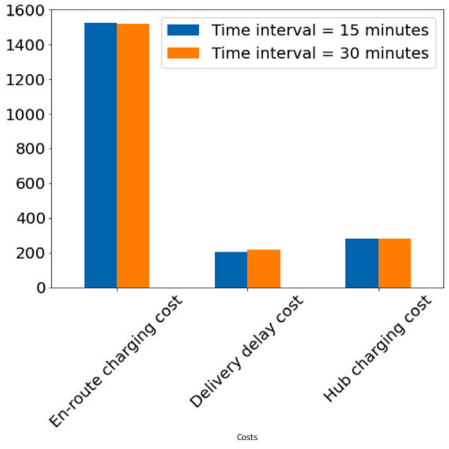

(e) Costs for different time-interval

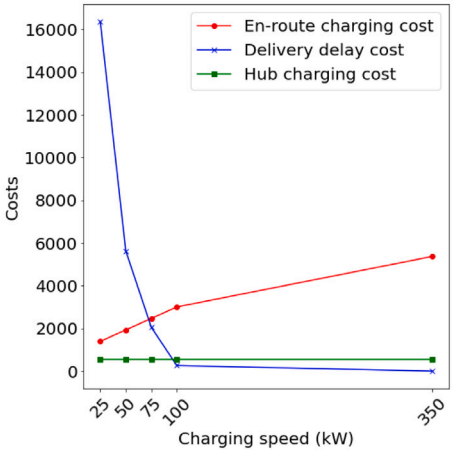

(f) Costs for different charging speeds of CSs

Fig. 6. Sensitivity analysis.

Number of CSs. The impacts of different numbers of CSs on system costs are illustrated in Fig. 6(c). We found that with the increase of CSs, delivery delay costs decreased slightly. The reason is that when there are more CSs, EFVs have more flexibility to charge

their vehicles and join a platoon. Therefore, EFVs do not need to wait as long before joining a platoon and less delay occurred to reach the destination. But since the amount of total energy consumption is similar regardless of the number of CS and EFVs will still prefer to charge as less as possible en-route, the en-route charging costs and the hub charging costs were almost the same for the different number of charging stations.

Capacity of CSs. The impacts of the capacitated en-route CSs and uncapacitated en-route CSs on system costs are illustrated in Fig. 6(d). We found that capacitated CSs increased delivery delay costs and en-route charging costs, while the hub charging cost had no change. The increased delivery delay costs and en-route charging costs are related. The reason is that capacitated CSs limit the flexibility to charge when all the charging plugs at a CS are occupied. In such a situation, an EFV may need to choose another CS, which reduces their chance to join platoons to save energy. Travel alone increases the total energy consumption and leads to more en-route charging needs and en-route charging time, which leads to an increase in en-route charging costs and delivery delay costs.

Time-interval. The impact of time-interval length is illustrated in Fig. 6(e). We find that 15-min and 30-min time intervals do not result in a significant difference in en-route charging and delivery delay cost. However, in terms of computational time, our model with a 15-min time-interval takes 1.5 h to solve, which is 3 times longer than a model with a 30-min time-interval. This is as expected as the smaller time-interval length makes the model much larger in terms of the number of variables and constraints.

Maximum SOC. The case with a 100% SOC cap is a relaxation of the case with a 80% SOC cap (i.e., the feasible region of the "80%" SOC case is a subset of the feasible region of the "100%" SOC case). Therefore, the objective value of the "80%" SOC case is no less than the "100%" SOC case. In this numerical example, we find that these two cases have exactly the same costs, which indicates that all EFVs do not need to be charged over 80% SOC to achieve better cost savings in terms of energy costs and delay costs.

Charging speed. The impacts of different charging speeds of en-route charging stations on system costs are illustrated in Fig. 6(f). The charging cost per kWh was also updated as \$0.50, \$0.28, \$0.23, \$0.18, and \$0.13 per kW for charging speeds of 350, 100, 75, 50, and 25 kW, respectively. We found that although a higher charging speed slightly increased the en-route charging cost, it significantly reduced the delivery delay cost. For example, by increasing the charging speed from 25 kW to 50 kW, we observed a 70% reduction in the delivery delay cost. When the charging speed is 350 kW, the delivery delay cost becomes zero. However, notice that the charging costs increase with the charging speed, the en-route charging cost increases 78% compared with 100 kW charging speed. Due to such a higher en-route charging cost, the total cost increases 55%. This is as expected because EFVs spend less time charging with a higher charging speed and are more likely to deliver on time. This result indicates that although the charging cost is less for lower-speed chargers, it is not wise to charge EFVs with such chargers when EFVs have a tight delivery schedule. The hub charging cost was constant because regardless of charging speed, EFVs would only charge for the minimum energy at en-route CSs since hub charging was cheaper in our numerical setting.

5. Discussion

This study proposes an MILP model for the scheduling of charging and platooning in the context of long-haul electric freight transportation. The model minimizes the total costs including en-route charging, delivery delay, and hub charging costs. With numerical examples and sensitivity analyses using a selected long-haul route in the Florida freight network, we found that:

- Each vehicle needed to charge 3–6 times and most charging demand was fulfilled 3–9 h after departure from origin.
- Most long-haul EFVs can leverage the charging activities to platoon together when sufficient charging plugs are available while platooning can reduce the total energy consumption and reduce en-route charging needs, which improves on-time delivery.
- The increase of CSs, charging plugs, charging speed, and model-decided departure time can reduce the delay cost, while high-performance EFVs with better battery capacity and energy efficiency can reduce the en-route charging cost.
- Compared with dynamic search and Bender's decomposition algorithms, the branch-and-cut algorithm with tuned parameters has the best computational performance for the proposed model.

This paper can be extended in several directions. First, we only consider one long-haul route and single OD pair for this study. The consideration of multiple ODs from a network perspective can be a valuable next step for future research. Second, the proposed model can be naturally extended to a stochastic version to consider system uncertainties, such as travel delay due to traffic restrictions, accidents, or vehicle failures, charging availability, and queuing time, which will further increase the scheduling reliability. Third, for large-scale network-level scheduling problems with a high dimension of uncertainties and a larger number of EFVs, one can design customized algorithms based on decomposition and approximation to further enhance computational efficiency.

Algorithm 1 Pseudo-code for Benders' decomposition Algorithm

Let UB and LB be upper bound and lower bound, respectively.
Initialization: $UB \leftarrow +\infty$
Solve the master problem: $LB \leftarrow Objective\ Function$
while $UB - LB \geq 0.01$ **do**
    Solve subproblem (SP)
    if SP is infeasible **then**
        Add slack variables to coupling constraints
        Augment the objective function with penalty multiplier with each slack variable
        Resolve the SP
    end if
    if SP is feasible **then**
        Update UB. $UB := min(current\ UB, \sum(objective\ value\ of\ SP\ and\ MP))$
        Find the dual of constraints of SP
        Add benders' (i.e., optimality) cut to MP
    end if
    Solve MP
    Update LB:$LB \leftarrow Objective\ Function$
end while

Algorithm 2 Pseudo-code for Branch and Cut Algorithm

Let x^* is optimal solution and v^* is the best objective value, respectively.
Initialization: x^*=null and v^*=$+\infty$
Add the initial MILP to $\mathcal{L}$, the set of active problems
while $\mathcal{L}$ is not empty **do**
    Select and remove (de-queue) a problem from $\mathcal{L}$
    Solve LP relaxation of the problem
    if The solution is infeasible **then**
        Go back to line 4
    else
        Denote the solution by x with objective value v
    end if
    if $v \geq v^*$ **then**
        Go back to line 4
    else
        if x is Integer **then**
            Set $v^* \leftarrow v$ and $x^* \leftarrow x$
            Go back to line 4
        end if
    end if
    Search for cutting planes that are violated by x
    if Cutting planes are found **then**
        Add them to the LP relaxation
        Go back to line 6
    else
        Branch to partition the problem into new problems with restricted feasible regions.
        Add these problems to $\mathcal{L}$ and go back to line 4
    end if
end while
return x^*

CRediT authorship contribution statement

Md Rakibul Alam: Methodology, Formal analysis, Investigation, Writing – original draft, Writing – review & editing. **Zhaomiao Guo:** Conceptualization, Methodology, Supervision, Writing – review & editing.

Acknowledgments

The efforts of Zhaomiao Guo are partially supported by the National Science Foundation, United States under Grant No. 2041446. The U.S. Government assumes no liability for the contents or use thereof. Freight data collection and processing are supported by UCF Office of Research Seed Funding. We also acknowledge Muhammad Shahbaz for initial data pre-processing for this research.

Appendix A. Benders decomposition algorithm

See Algorithm 1.

Appendix B. Branch and cut algorithm

See Algorithm 2.

References

Alam, A., 2014. Fuel-Efficient Heavy-Duty Vehicle Platooning (Ph.D. thesis). KTH Royal Institute of Technology.
Andelmin, J., Bartolini, E., 2017. An exact algorithm for the green vehicle routing problem. Transp. Sci. 51 (4), 1288–1303.
Anderluh, A., Nolz, P.C., Hemmelmayr, V.C., Crainic, T.G., 2021. Multi-objective optimization of a two-echelon vehicle routing problem with vehicle synchronization and 'grey zone'customers arising in urban logistics. European J. Oper. Res. 289 (3), 940–958.
Basso, R., Kulcsár, B., Egardt, B., Lindroth, P., Sanchez-Diaz, I., 2019. Energy consumption estimation integrated into the electric vehicle routing problem. Transp. Res. D 69, 141–167.
Bischoff, J., Márquez-Fernández, F.J., Domingues-Olavarría, G., Maciejewski, M., Nagel, K., 2019. Impacts of vehicle fleet electrification in Sweden–a simulation-based assessment of long-distance trips. In: 2019 6th International Conference on Models and Technologies for Intelligent Transportation Systems (MT-ITS). IEEE, pp. 1–7.
Bonnet, C., Fritz, H., 2000. Fuel Consumption Reduction in a Platoon: Experimental Results with Two Electronically Coupled Trucks at Close Spacing. Technical Report, SAE technical paper.
Bosona, T., 2020. Urban freight last mile logistics—challenges and opportunities to improve sustainability: a literature review. Sustainability 12 (21), 8769.
Bruni, M., Jabali, O., Khodaparasti, S., 2020. The electric vehicle route planning problem with energy consumption uncertainty. In: 2020 Forum on Integrated and Sustainable Transportation Systems (FISTS). IEEE, pp. 224–229.
Chen, T.D., Kockelman, K.M., Khan, M., 2013. Locating electric vehicle charging stations: Parking-based assignment method for Seattle, Washington. Transp. Res. Rec. 2385 (1), 28–36.
Dalmijn, M., Atasoy, B., Bijl, P., Negenborn, R.R., 2020. Charge scheduling of electric vehicles for last-mile distribution of an e-grocer. In: 2020 Forum on Integrated and Sustainable Transportation Systems (FISTS). IEEE, pp. 236–241.
Davila, A., Aramburu, E., Freixas, A., 2013. Making the best out of aerodynamics: Platoons. In: SAE 2013 World Congress & Exhibition.
Desaulniers, G., Errico, F., Irnich, S., Schneider, M., 2016. Exact algorithms for electric vehicle-routing problems with time windows. Oper. Res. 64 (6), 1388–1405.
EPA, 2018. Fast fast U.S.transportation sector greenhouse gas emissions 1990 –2016. URL: https://nepis.epa.gov/Exe/ZyPDF.cgi?Dockey=P100USI5.pdf.
FDOT, 2022. Container number database. URL: https://www.fdot.gov/docs/default-source/statistics/multimodaldata/multimodal/Container-Number-Database-(CNDB).pdf.
FMCSA, 2022. Hours of service (HOS). URL: https://www.fmcsa.dot.gov/regulations/hours-of-service.
Gounaris, C.E., Repoussis, P.P., Tarantilis, C.D., Floudas, C.A., 2011. A hybrid branch-and-cut approach for the capacitated vehicle routing problem. In: Pistikopoulos, E., Georgiadis, M., Kokossis, A. (Eds.), 21st European Symposium on Computer Aided Process Engineering. In: Computer Aided Chemical Engineering, 29, Elsevier, pp. 507–511. http://dx.doi.org/10.1016/B978-0-444-53711-9.50102-4, URL: https://www.sciencedirect.com/science/article/pii/B9780444537119501024.
Hiermann, G., Puchinger, J., Ropke, S., Hartl, R.F., 2016. The electric fleet size and mix vehicle routing problem with time windows and recharging stations. European J. Oper. Res. 252 (3), 995–1018.
İmre, Ş., Çelebi, D., Koca, F., 2021. Understanding barriers and enablers of electric vehicles in urban freight transport: Addressing stakeholder needs in Turkey. Sustainable Cities Soc. 68, 102794.
Kavianipour, M., Fakhrmoosavi, F., Singh, H., Ghamami, M., Zockaie, A., Ouyang, Y., Jackson, R., 2021. Electric vehicle fast charging infrastructure planning in urban networks considering daily travel and charging behavior. Transp. Res. D 93, 102769.
Klumpp, M., Witte, C., Zelewski, S., 2014. Information and process requirements for electric mobility in last-mile-logistics. In: Information Technology in Environmental Engineering. Springer, pp. 201–208.
Lammert, M., 2020. Truck platooning: Fuel-saving assessments. URL: https://www.nrel.gov/transportation/fleettest-platooning.html.
Lammert, M.P., Bugbee, B., Hou, Y., Muratori, M., Holden, J., Duran, A.W., Mack, A., Swaney, E., 2018. Exploring Telematics Big Data for Truck Platooning Opportunities. Technical Report, National Renewable Energy Lab.(NREL), Golden, CO (United States).
Lee, W.J., Kwag, S.I., Ko, Y.D., 2021. The optimal eco-friendly platoon formation strategy for a heterogeneous fleet of vehicles. Transp. Res. D 90, 102664.
Liu, P., Wang, C., Fu, T., Guan, Z., 2019. Efficient electric vehicles assignment for platoon-based charging. In: 2019 IEEE Wireless Communications and Networking Conference (WCNC). IEEE, pp. 1–6.
Macrina, G., Pugliese, L.D.P., Guerriero, F., Laporte, G., 2019. The green mixed fleet vehicle routing problem with partial battery recharging and time windows. Comput. Oper. Res. 101, 183–199.
Michaelian, M., Browand, F., et al., 2000. Field experiments demonstrate fuel savings for close-following, California PATH Program, Institute of Transportation Studies. University of California At Berkeley.
MIT, 2021. Freight transportation. URL: https://climate.mit.edu/explainers/freight-transportation.
Morrissey, P., Weldon, P., O'Mahony, M., 2016. Future standard and fast charging infrastructure planning: An analysis of electric vehicle charging behaviour. Energy Policy 89, 257–270.
Nykvist, B., Olsson, O., 2021. The feasibility of heavy battery electric trucks. Joule 5 (4), 901–913.
Osieczko, K., Zimon, D., Płaczek, E., Prokopiuk, I., 2021. Factors that influence the expansion of electric delivery vehicles and trucks in EU countries. J. Environ. Manag. 296, 113177.
Pelletier, S., Jabali, O., Laporte, G., 2019. The electric vehicle routing problem with energy consumption uncertainty. Transp. Res. B 126, 225–255.
Schneider, M., Stenger, A., Goeke, D., 2014. The electric vehicle-routing problem with time windows and recharging stations. Transp. Sci. 48 (4), 500–520.

Sen, B., Ercan, T., Tatari, O., 2017. Does a battery-electric truck make a difference?–Life cycle emissions, costs, and externality analysis of alternative fuel-powered Class 8 heavy-duty trucks in the United States. J. Clean. Prod. 141, 110–121.

Siddique, C., Afifah, F., Guo, Z., Zhou, Y., 2022. Data mining of plug-in electric vehicles charging behavior using supply-side data. Energy Policy 161, 112710.

Smith, D., Ozpineci, B., Graves, R.L., Jones, P., Lustbader, J., Kelly, K., Walkowicz, K., Birky, A., Payne, G., Sigler, C., et al., 2020. Medium-And Heavy-Duty Vehicle Electrification: An Assessment of Technology and Knowledge Gaps. Technical Report, Oak Ridge National Lab.(ORNL), Oak Ridge, TN (United States).

Taefi, T.T., Kreutzfeldt, J., Held, T., Fink, A., 2016. Supporting the adoption of electric vehicles in urban road freight transport–A multi-criteria analysis of policy measures in Germany. Transp. Res. A 91, 61–79.

Tsugawa, S., 2013. An overview on an automated truck platoon within the energy ITS project. IFAC Proc. Vol. 46 (21), 41–46.

Vijayagopal, R., Rousseau, A., 2021. Electric truck economic feasibility analysis. World Electr. Veh. J. 12 (2), 75.

Wang, M., van Maarseveen, S., Happee, R., Tool, O., van Arem, B., 2019. Benefits and risks of truck platooning on freeway operations near entrance ramp. Transp. Res. Rec. 2673 (8), 588–602.

Xie, F., Lin, Z., 2021. Integrated US nationwide corridor charging infrastructure planning for mass electrification of inter-city trips. Appl. Energy 298, 117142.

Zhang, J., Tang, T.-Q., Yan, Y., Qu, X., 2021. Eco-driving control for connected and automated electric vehicles at signalized intersections with wireless charging. Appl. Energy 282, 116215.

Zhao, Z., Fan, L., Han, Z., 2021. Hybrid quantum benders' decomposition for mixed-integer linear programming. arXiv preprint arXiv:2112.07109.

Zhou, Y., Rood, M., 2019. National Energy Impacts of Heavy Electric Truck Adoption For Freight. Technical Report, Argonne National Lab.(ANL), Argonne, IL (United States).